

Drell-Yan Non-Singlet Spin Cross Sections and Spin Asymmetry to $O(\alpha_s^2)$ (II)

Sanghyeon Chang^{*1}, Claudio Corianò^{**2} and R. D. Field^{*3}

** Institute for Fundamental Theory, Department of Physics,
University of Florida, Gainesville, FL 32611, USA*

*** Jefferson Lab, Newport News, VA, 23606, USA*

Abstract

We present predictions for the non-singlet Drell-Yan longitudinal spin cross sections and spin asymmetry, A_{LL} , in proton-proton collisions at large p_T at the RHIC energy of 200 GeV at next-to-leading order QCD. The higher order corrections to the non-singlet polarized cross section, σ_{NS}^{LL} , are sizeable and similar to those found for the unpolarized cross section. The non-singlet asymmetry parameter, A_{LL}^{NS} , is very stable against higher order corrections and is a direct measurement of the non-singlet (*i.e.*, valence) polarized quark distributions within the proton.

¹ E-mail address: schang@phys.ufl.edu

² E-mail address: coriano@jlab2.jlab.org

³ E-mail address: rfield@phys.ufl.edu

1 Introduction

The study of the spin content of the nucleon at hadron/hadron colliders is one of the most interesting aspects of QCD which is increasing receiving attention both from the theoretical and from the experimental side.

Among the most interesting questions that a p - p collider can help us answer is the issue of the distribution of the proton spin among its constituents and the measurement of various polarized parton distributions. In this new setting, the presence of a direct gluon coupling, absent in polarized Deep Inelastic scattering processes, will allow a direct test of the gluon contribution to the polarization of the nucleon, with measurements covering a wide x (Bjorken- x) range. We mention that, especially at smaller x values, the gluon polarization ΔG is strongly model-dependent and, therefore, poorly known from DIS experiments alone.

Along these lines, in the last few years, several studies regarding the analysis of the scaling violations in polarized p - p collisions have been presented, and considerable progress has been made in the theoretical investigation of various important polarized processes. For instance, it has become now clear that inclusive prompt photon production [1] ($p p \rightarrow \gamma + X$), photon-plus-jet production ($p p \rightarrow \gamma + J$) [2], and polarized production of 2 jets ($p p \rightarrow J J$) are among the most important processes to be studied at RHIC, the Relativistic Heavy Ion Collider at Brookhaven.

The corresponding cross sections show sizable asymmetries (see for instance [3]) with good hope for the experimental program. We mention also that, beside the usual asymmetries for total cross sections or large p_T cross sections, other observables of the final state can be used as a way to test the size and the sign of ΔG .

In this respect, the study of the event-structure of the final state and the asymmetries for various correlations (for instance rapidity correlations, angular correlations in the photon/jet system) have been shown also to be a source of important information on the polarized parton distributions and can help us discriminate among the various different models [3].

More recently, lepton pair production via the Drell-Yan mechanism has also received considerable attention. The process has been historically a clean way to test QCD and the parton model and continues to be so also in the case of polarized collisions. In a seminal paper [4], Ralston and Soper pointed out that the factorization formula for parton distributions for Drell-Yan includes, beside the usual longitudinally polarized parton distributions, also parton distributions for transverse spin. In particular the study of the transverse spin distribution is one of the challenging tasks that the STAR and PHENIX collaborations at RHIC are going to undertake within the next few years.

On the technical side, we remind that although formal proofs of factorization are still missing, direct calculations show that the Drell-Yan cross sections does factorize, as shown in nontrivial cases (for instance for the nonzero p_T distributions [5]). This opens the way to an accurate study of this important cross section both for longitu-

dinal and transverse spin. At $p_T = 0$, where p_T describes the transverse momentum of the lepton pair, the calculations simplify drastically and various results have been reported in the literature (see for instance [7, 8] for the longitudinal case).

In previous works [6], we have analyzed the spin dependence of hard scattering in Drell-Yan (with longitudinal polarization) at parton level to NLO QCD, at nonzero p_T of the lepton pair. In this work we proceed with the analysis at hadron level of these former results, thereby providing predictions for the behavior of the cross section at RHIC energies. Since our NLO analysis is limited to the non singlet sector, our study is exploratory in nature, and we have limited our attention to just one particular center of mass scattering energy (200 GeV), right in the middle of the planned RHIC energy range. We will also limit our interest to a single set of parton distributions, specified below. Our interest, in this work, is limited to assess the stability of the full $O(\alpha_s^2)$ calculation, predict the asymmetries of various helicity dependent amplitudes and show that the corresponding K factors are comparable to the unpolarized ones.

The asymmetries turn out to be sizable and can be larger than what estimated here once the gluon contribution is fully included. We hope to return to a re-analysis of the complete process in the near future.

2 Structure of the Differential Cross Section

We begin by examining the contribution to the production of *virtual* photons with invariant mass, Q , in hadron-hadron collisions,

$$H_1 + H_2 \rightarrow \gamma^* + X, \quad (1)$$

from the $2 \rightarrow 3$ parton subprocess,

$$a + b \rightarrow \gamma^* + c + d. \quad (2)$$

Here H_1 and H_2 are incoming hadrons with 4-momenta, P_1 and P_2 , respectively, and q is the 4-momentum of the virtual photon, γ^* , as shown in Fig. 1. The 4-momenta of the incoming two parton a and b are labeled by p_1 and p_2 respectively, and the outgoing 4-momenta of partons c and d are labeled by k_2 and k_3 . The virtual photon 4-momenta is given by $k_1 = q$. Conservation of energy and momentum implies that

$$p_1 + p_2 = k_1 + k_2 + k_3. \quad (3)$$

The hadron-hadron process (1) is described in terms of the invariants,

$$S = (P_1 + P_2)^2, \quad T = (P_1 - q)^2, \quad U = (P_2 - q)^2. \quad (4)$$

In addition, it is convenient to define the scaled variables

$$x_T = 2q_T/W \text{ and } \tau = Q^2/S, \quad (5)$$

where $W = \sqrt{S}$ is the hadron-hadron center-of-mass energy and q_T is the transverse momentum of the virtual photon with invariant mass, Q . It is also useful to define the following two quantities,

$$\bar{x}_1 = \frac{Q^2 - U}{S} = \frac{1}{2}e^y\sqrt{x_T^2 + 4\tau}, \quad \bar{x}_2 = \frac{Q^2 - T}{S} = \frac{1}{2}e^{-y}\sqrt{x_T^2 + 4\tau}, \quad (6)$$

where y is the rapidity of the virtual photon. The $2 \rightarrow 3$ parton subprocess (2) is described in terms of the invariants,

$$s = (p_1 + p_2)^2, \quad t = (p_1 - q)^2, \quad u = (p_2 - q)^2, \quad (7)$$

and

$$s_2 = s_{23} = (k_2 + k_3)^2, \quad (8)$$

where momentum and energy conservation (3) implies

$$s + t + u = Q^2 + s_2. \quad (9)$$

In QCD the hadronic cross section is related to the parton subprocess according to

$$d\sigma(H_1 + H_2 \rightarrow \gamma^* + X; W, q_T, y) = G_{H_1 \rightarrow a}(x_1, M^2)dx_1 G_{H_2 \rightarrow b}(x_2, M^2)dx_2 \left(\frac{d\hat{\sigma}}{dtdu}(ab \rightarrow \gamma^* cd; s, t, u) \right) dtdu, \quad (10)$$

where $G_{H_1 \rightarrow a}(x_1, M^2)dx_1$ is the number of partons of flavor a with momentum fraction, $x_1 = p_1/P_1$, within hadron H_1 at the factorization scale M . Similarly, $G_{H_2 \rightarrow b}(x_2, M^2)dx_2$ is the number of partons of flavor b with momentum fraction $x_2 = p_2/P_2$, within hadron H_2 , at the factorization scale M . In the remainder of this paper we will take the factorization scale to be Q and evaluate the parton subprocesses at the same scale Q . Using (4) and (7) we see that

$$s = x_1 x_2 S, \quad (11)$$

$$(t - Q^2) = x_1(T - Q^2) = -x_1 \bar{x}_2 S, \quad (12)$$

$$(u - Q^2) = x_2(U - Q^2) = -x_2 \bar{x}_1 S, \quad (13)$$

which from (9) implies that

$$x_1 x_2 - x_1 \bar{x}_2 - x_2 \bar{x}_1 = \tau_2 - \tau, \quad (14)$$

where \bar{x}_1 and \bar{x}_2 are defined in (6) and

$$\tau_2 = s_2/S. \quad (15)$$

It is now easy to compute the Jacobian

$$dx_2 dt = \frac{s}{4(x_1 - \bar{x}_1)} dx_T^2 dy, \quad (16)$$

which when inserted into (10) and integrating over x_1 and s_2 gives

$$S \frac{d\sigma}{dq_T^2 dy}(W, q_T, y) = \int_{x_1^{min}}^1 dx_1 \int_0^{s_2^{max}} ds_2 \frac{1}{(x_1 - \bar{x}_1)} G_{H_1 \rightarrow a}(x_1, Q^2) G_{H_2 \rightarrow b}(x_2, Q^2) s \frac{d\hat{\sigma}}{dt du}(ab \rightarrow \gamma^* cd; s, t, u), \quad (17)$$

where

$$x_2 = \frac{x_1 \bar{x}_2 + \tau_2 - \tau}{x_1 - \bar{x}_1}, \quad (18)$$

and

$$s_2^{max} = A = (\tau - \bar{x}_1 + x_1(1 - \bar{x}_2))S, \quad x_1^{min} = \frac{\bar{x}_1 - \tau}{1 - \bar{x}_2}. \quad (19)$$

The maximum value of τ_2 arises when $x_2 = 1$ in (14), while the minimum value of x_1 occurs when $\tau_2 = 0$ and $x_2 = 1$.

For $2 \rightarrow 2$ parton subprocesses such as the Born contribution in Fig. 2 one has

$$s \frac{d\hat{\sigma}}{dt du}(s, t, u) = \delta(s_2) s \frac{d\hat{\sigma}}{dt}(a + b \rightarrow \gamma^* + c; s, t), \quad (20)$$

which when inserted into (17) results in

$$S \frac{d\sigma}{dq_T^2 dy}(W, q_T, y) = \int_{x_1^{min}}^1 dx_1 \frac{1}{(x_1 - \bar{x}_1)} G_{H_1 \rightarrow a}(x_1, Q^2) G_{H_2 \rightarrow b}(x_2, Q^2) s \frac{d\hat{\sigma}}{dt}(ab \rightarrow \gamma^* c; s, t), \quad (21)$$

where in this case $s_2 = 0$ and $s + t + u = Q^2$.

The Drell-Yan differential cross section for producing a muon pair with transverse momentum q_T and invariant mass, Q , at rapidity y in the hadron-hadron collision,

$$H_1 + H_2 \rightarrow (\gamma^* \rightarrow \mu^+ \mu^-) + X, \quad (22)$$

at center-of-mass energy W , is given by

$$S \frac{d\sigma}{dQ^2 dq_T^2 dy}(H_1 H_2 \rightarrow \mu^+ \mu^- + X; W, Q^2, q_T, y) = \left(\frac{\alpha}{3\pi Q^2} \right) S \frac{d\sigma}{dq_T^2 dy}(H_1 H_2 \rightarrow \gamma^* + X; W, q_T, y), \quad (23)$$

where α is the electromagnetic fine structure constant and where the virtual photon differential cross section is given by (17) or (21).

2.1 The Non-Singlet Cross Section

We define the ‘‘non-singlet’’ cross section at the hadron level to be the antihadron-hadron minus the hadron-hadron cross section as follows:

$$\sigma_{NS} = \sigma_{\overline{H}_1 H_2} - \sigma_{H_1 H_2}, \quad (24)$$

and at the parton level to be the quark-antiquark minus the quark-quark cross section,

$$\hat{\sigma}_{NS} = \hat{\sigma}_{q\bar{q}} - \hat{\sigma}_{qq}. \quad (25)$$

Since the antihadron-hadron cross section is larger, this definition yields positive values for σ_{NS} . For parton distributions, on the other hand, we use the customary non-singlet definition,

$$G_{H \rightarrow q}^{NS} = G_{H \rightarrow q} - G_{H \rightarrow \bar{q}}. \quad (26)$$

In proton-proton collisions the non-singlet cross section is given by

$$\begin{aligned} \sigma_{pp}^{NS} &= \sigma_{\bar{p}p} - \sigma_{pp} \\ &= (G_{\bar{p} \rightarrow q} G_{p \rightarrow q} + G_{\bar{p} \rightarrow \bar{q}} G_{p \rightarrow \bar{q}}) \otimes \hat{\sigma}_{qq} \\ &\quad + (G_{\bar{p} \rightarrow q} G_{p \rightarrow \bar{q}} + G_{\bar{p} \rightarrow \bar{q}} G_{p \rightarrow q}) \otimes \hat{\sigma}_{q\bar{q}} \\ &\quad - (G_{p \rightarrow q} G_{p \rightarrow q} + G_{p \rightarrow \bar{q}} G_{p \rightarrow \bar{q}}) \otimes \hat{\sigma}_{qq} \\ &\quad - (G_{p \rightarrow q} G_{p \rightarrow \bar{q}} + G_{p \rightarrow \bar{q}} G_{p \rightarrow q}) \otimes \hat{\sigma}_{q\bar{q}} \\ &= G_{p \rightarrow q}^{NS} G_{p \rightarrow q}^{NS} \otimes \hat{\sigma}_{qq}^{NS}, \end{aligned} \quad (27)$$

where the convolution \otimes is defined in (17) and (21).

2.2 The Spin Dependent Cross Sections

The non-singlet proton-proton helicity dependent Drell-Yan cross section can be written in the form,

$$\begin{aligned} S \frac{d\sigma_{NS}}{dQ^2 dq_T^2 dy} (W, Q^2, q_T, y, \Lambda_1, \Lambda_2) &= \\ &\left(\frac{\alpha}{3\pi Q^2} \right) \sum_q \sum_{\lambda_1, \lambda_2} \int_{x_1^{min}}^1 dx_1 \int_0^{s_2^{max}} ds_2 \frac{1}{(x_1 - \bar{x}_1)} \\ &G_{p[\Lambda_1] \rightarrow q[\lambda_1]}^{NS}(x_1, Q^2) G_{p[\Lambda_2] \rightarrow q[\lambda_2]}^{NS}(x_2, Q^2) s \frac{d\hat{\sigma}_{NS}}{dt du}(s, t, u, h), \end{aligned} \quad (28)$$

where Λ_1 and Λ_2 are the helicities of the initial two hadrons, respectively, and $h = 4\lambda_1\lambda_2$. In 28 the sum is over the quark flavor and the quark helicities λ_1 and λ_2 , while the non-singlet helicity structure functions are given by

$$G_{p[\Lambda] \rightarrow q_f[\lambda]}^{NS} = G_{p[\Lambda] \rightarrow q_f[\lambda]} - G_{p[\Lambda] \rightarrow \bar{q}_f[\lambda]}. \quad (29)$$

For one quark flavor

$$\begin{aligned}\sigma_{++}^{NS} &= \left(G_{\uparrow\rightarrow\uparrow}^{NS} G_{\uparrow\rightarrow\uparrow}^{NS} + G_{\uparrow\rightarrow\downarrow}^{NS} G_{\uparrow\rightarrow\downarrow}^{NS} \right) \otimes \hat{\sigma}_{++}^{NS} \\ &+ \left(G_{\uparrow\rightarrow\uparrow}^{NS} G_{\uparrow\rightarrow\downarrow}^{NS} + G_{\uparrow\rightarrow\downarrow}^{NS} G_{\uparrow\rightarrow\uparrow}^{NS} \right) \otimes \hat{\sigma}_{+-}^{NS},\end{aligned}\quad (30)$$

and

$$\begin{aligned}\sigma_{+-}^{NS} &= \left(G_{\uparrow\rightarrow\uparrow}^{NS} G_{\downarrow\rightarrow\uparrow}^{NS} + G_{\uparrow\rightarrow\downarrow}^{NS} G_{\downarrow\rightarrow\downarrow}^{NS} \right) \otimes \hat{\sigma}_{++}^{NS} \\ &+ \left(G_{\uparrow\rightarrow\uparrow}^{NS} G_{\downarrow\rightarrow\downarrow}^{NS} + G_{\uparrow\rightarrow\downarrow}^{NS} G_{\downarrow\rightarrow\uparrow}^{NS} \right) \otimes \hat{\sigma}_{+-}^{NS},\end{aligned}\quad (31)$$

where \uparrow and \downarrow refer to helicity $+\frac{1}{2}$ and $-\frac{1}{2}$, respectively, and where we have used simplified ‘‘convolution notation’’. The unpolarized non-singlet cross section is the average of σ_{++}^{NS} and σ_{+-}^{NS} ,

$$\sigma_{NS}^{\Sigma} = \frac{1}{2} \left(\sigma_{++}^{NS} + \sigma_{+-}^{NS} \right), \quad (32)$$

while the non-singlet longitudinal spin difference (*i.e.*, polarized) cross section is defined by,

$$\sigma_{NS}^{LL} = \frac{1}{2} \left(\sigma_{++}^{NS} - \sigma_{+-}^{NS} \right). \quad (33)$$

From (30) and (31) it is easy to show that, for one quark flavor,

$$\sigma_{NS}^{\Sigma} = \left(G_{p\rightarrow q}^{NS} G_{p\rightarrow q}^{NS} \right) \otimes \hat{\sigma}_{NS}^{\Sigma}, \quad (34)$$

and

$$\sigma_{NS}^{LL} = \left(\Delta G_{p\rightarrow q}^{NS} \Delta G_{p\rightarrow q}^{NS} \right) \otimes \hat{\sigma}_{NS}^{LL}, \quad (35)$$

where the unpolarized parton distributions is the sum of the two spin states,

$$G_{p\rightarrow q}^{NS} = G_{\uparrow\rightarrow\uparrow}^{NS} + G_{\uparrow\rightarrow\downarrow}^{NS}, \quad (36)$$

and the ‘‘polarized’’ parton distributions is the difference of the two spin states,

$$\Delta G_{p\rightarrow q}^{NS} = G_{\uparrow\rightarrow\uparrow}^{NS} - G_{\uparrow\rightarrow\downarrow}^{NS}. \quad (37)$$

Similarly, the parton unpolarized non-singlet cross section is the average of $\hat{\sigma}_{++}^{NS}$ and $\hat{\sigma}_{+-}^{NS}$,

$$\hat{\sigma}_{NS}^{\Sigma} = \frac{1}{2} \left(\hat{\sigma}_{++}^{NS} + \hat{\sigma}_{+-}^{NS} \right), \quad (38)$$

and the polarized parton non-singlet cross section is defined by,

$$\hat{\sigma}_{NS}^{LL} = \frac{1}{2} \left(\hat{\sigma}_{++}^{NS} - \hat{\sigma}_{+-}^{NS} \right). \quad (39)$$

In Ref.[6] we showed that to order α_s^2 the Drell-Yan non-singlet spin-dependent parton-parton differential in (28) can be written as the Born term plus four (*unpolarized*) cross sections as follows:

$$\begin{aligned}s \frac{d\hat{\sigma}_{NS}}{dtdu}(s, t, u, h) &= (1-h)\delta(s_2)s \frac{d\hat{\sigma}_B^{\Sigma}}{dt} \\ &+ (1-h)s \frac{d\hat{\sigma}_1^{\Sigma}}{dtdu} + (1-h)s \frac{d\hat{\sigma}_2^{\Sigma}}{dtdu} + (1-h)s \frac{d\hat{\sigma}_3^{\Sigma}}{dtdu} - (1+h)s \frac{d\hat{\sigma}_4^{\Sigma}}{dtdu},\end{aligned}\quad (40)$$

where $h = 4\lambda_1\lambda_2$. Hence, to order α_s^2 the Drell-Yan non-singlet unpolarized differential cross section for producing muon pair with transverse momentum q_T and invariant mass, Q , at rapidity y in the proton-proton collision at center-of-mass energy, W , is given by,

$$S \frac{d\sigma^\Sigma}{dQ^2 dq_T^2 dy}(W, Q^2, q_T, y) = \left(\frac{\alpha}{3\pi Q^2}\right) \sum_{q=u,d} \int_{x_1^{\min}}^1 dx_1 \int_0^{s_2^{\max}} ds_2 \frac{1}{(x_1 - \bar{x}_1)} G_{p \rightarrow q}^{NS}(x_1, Q^2) G_{p \rightarrow q}^{NS}(x_2, Q^2) s \frac{d\hat{\sigma}_{NS}^\Sigma}{dtdu}(s, t, u), \quad (41)$$

where

$$s \frac{d\hat{\sigma}_{NS}^\Sigma}{dtdu}(s, t, u) = \delta(s_2) s \frac{d\hat{\sigma}_B^\Sigma}{dt} + s \frac{d\tilde{\sigma}_1^\Sigma}{dtdu} + s \frac{d\hat{\sigma}_2^\Sigma}{dtdu} + s \frac{d\hat{\sigma}_3^\Sigma}{dtdu} - s \frac{d\hat{\sigma}_4^\Sigma}{dtdu}, \quad (42)$$

and the polarized cross section is given by,

$$S \frac{d\sigma^{LL}}{dQ^2 dq_T^2 dy}(W, Q^2, q_T, y) = \left(\frac{\alpha}{3\pi Q^2}\right) \sum_{q=u,d} \int_{x_1^{\min}}^1 dx_1 \int_0^{s_2^{\max}} ds_2 \frac{1}{(x_1 - \bar{x}_1)} \Delta G_{p \rightarrow q}^{NS}(x_1, Q^2) \Delta G_{p \rightarrow q}^{NS}(x_2, Q^2) s \frac{d\hat{\sigma}_{NS}^{LL}}{dtdu}(s, t, u), \quad (43)$$

where

$$s \frac{d\hat{\sigma}_{NS}^{LL}}{dtdu}(s, t, u) = -\delta(s_2) s \frac{d\hat{\sigma}_B^\Sigma}{dt} - s \frac{d\tilde{\sigma}_1^\Sigma}{dtdu} - s \frac{d\hat{\sigma}_2^\Sigma}{dtdu} - s \frac{d\hat{\sigma}_3^\Sigma}{dtdu} - s \frac{d\hat{\sigma}_4^\Sigma}{dtdu}. \quad (44)$$

The unpolarized Born term, $\hat{\sigma}_B^\Sigma$ and the four *spin averaged* cross sections, $\tilde{\sigma}_1^\Sigma$, $\hat{\sigma}_2^\Sigma$, $\hat{\sigma}_3^\Sigma$, and $\hat{\sigma}_4^\Sigma$, are given in Ref.[6] and Ref.[10].

3 Proton-Proton Collisions at 200 GeV

3.1 Polarized and Unpolarized Cross Sections

To illustrate the effect of the higher order terms in muon-pair production in hadron-hadron collisions, we compute the non-singlet polarized and unpolarized Drell-Yan cross sections in proton-proton collisions at $W = 200$ GeV. The non-singlet unpolarized cross section is given by (41), which in convolution notation becomes

$$\sigma_{NS}^\Sigma = \sum_{q=u,d} \left(G_{p \rightarrow q}^{NS} G_{p \rightarrow q}^{NS} \right) \otimes \hat{\sigma}_{NS}^\Sigma, \quad (45)$$

where from (42)

$$\hat{\sigma}_{NS}^{\Sigma} = \hat{\sigma}_B + \tilde{\sigma}_1 + \hat{\sigma}_2 + \hat{\sigma}_3 - \hat{\sigma}_4. \quad (46)$$

The non-singlet longitudinal (*polarized*) cross section given by (43) becomes

$$\sigma_{NS}^{LL} = \sum_{q=u,d} \left(\Delta G_{p \rightarrow q}^{NS} \Delta G_{p \rightarrow q}^{NS} \right) \otimes \hat{\sigma}_{NS}^{LL}, \quad (47)$$

where from (44)

$$\hat{\sigma}_{NS}^{LL} = -\hat{\sigma}_B - \tilde{\sigma}_1 - \hat{\sigma}_2 - \hat{\sigma}_3 - \hat{\sigma}_4. \quad (48)$$

We use GS solution A [9] for the polarized and unpolarized parton distributions ($\Lambda = 200$ MeV) which are shown in Fig. 3 at $Q = 2$ GeV. Fig. 4 shows the polarized and unpolarized non-singlet cross sections to leading order (*Born term*) and to order α_s^2 at $W = 200$ GeV, $Q = M = 2$ GeV, and $y = 0$. Fig. 4 shows the “number density” $dN/d\tau dx_T dy$ which is constructed from the cross section as follows:

$$\frac{d\sigma}{d\tau dx_T dy} = \frac{x_T}{2} S^2 \frac{d\sigma}{dQ^2 dq_T^2 dy}, \quad (49)$$

using an integrated luminosity of 100/pb.

Fig. 5 shows the non-singlet polarized and unpolarized cross sections to leading order and to order α_s^2 at $W = 200$ GeV and $Q = M = 2$ GeV integrated over y

$$\frac{d\sigma}{d\tau dx_T} = \int_{y_{min}}^{y_{max}} \frac{d\sigma}{d\tau dx_T dy} dy. \quad (50)$$

Here the number density $dN/d\tau dx_T$ corresponds to the number of events per unit τ per unit x_T in 100/pb. To compute the number of events in a bin of τ of size 0.0001 (corresponding to $\Delta M = 2$ GeV at $W = 200$ GeV) and a bin of x_T of size 0.01 (corresponding to $\Delta p_T = 1$ GeV at $W = 200$ GeV), for example, one would multiply $dN/d\tau dx_T$ by 10^{-6} .

Fig. 6 and Fig. 7 show the ratio of the full order α_s^2 to the leading order cross sections (*i.e.*, the “K-factors”) for the polarized and unpolarized case. As has been previously seen, the K-factor for the unpolarized cross section is quite large. The polarized K-factor is almost the same as the unpolarized case. The difference comes only from $\hat{\sigma}_4$ in (46) and (48) and from the fact that the polarized and unpolarized parton distributions are different. However, the contribution to the cross sections from $\hat{\sigma}_4$ are small, as can be seen in Fig. 8 and Fig. 9, which show the individual K-factors arising from the four terms in (46) for the unpolarized cross section and from the four terms in (48) for the polarized cross section, respectively. For both the polarized and unpolarized case the dominant term in the K-factor is $\tilde{\sigma}_1$.

3.2 Spin Cross Sections

The spin cross sections σ_{++}^{NS} and σ_{+-}^{NS} are calculated from σ_{NS}^{Σ} and σ_{NS}^{LL} as follows:

$$\begin{aligned}\sigma_{++}^{NS} &= \sigma_{NS}^{\Sigma} + \sigma_{NS}^{LL}, \\ \sigma_{+-}^{NS} &= \sigma_{NS}^{\Sigma} - \sigma_{NS}^{LL},\end{aligned}\tag{51}$$

and are shown in Fig. 10. To leading order at the parton level,

$$\hat{\sigma}_{++}^{NS} = 0 \quad (\text{leading order}),\tag{52}$$

which from (30) - at the hadron level - implies an ‘‘indirect’’ contribution of the form

$$\sigma_{++}^{NS} = 2 \sum_{u,d} \left(G_{\uparrow\rightarrow\uparrow}^{NS} G_{\uparrow\rightarrow\downarrow}^{NS} + G_{\uparrow\rightarrow\downarrow}^{NS} G_{\uparrow\rightarrow\uparrow}^{NS} \right) \otimes \hat{\sigma}_{NS}^{\Sigma} \quad (\text{leading order}),\tag{53}$$

where

$$\hat{\sigma}_{NS}^{\Sigma} = \hat{\sigma}_B \quad (\text{leading order}).\tag{54}$$

Fig. 11 shows that the probability of finding a quark carrying helicity opposite to that of the proton ($G_{\uparrow\rightarrow\downarrow}$ or $G_{\downarrow\rightarrow\uparrow}$) is not small especially at small x and hence at the hadron level σ_{++}^{NS} is not zero.

At order α_s^2 ,

$$\begin{aligned}\sigma_{++}^{NS} &= -2 \sum_{u,d} \left(G_{\uparrow\rightarrow\uparrow}^{NS} G_{\uparrow\rightarrow\uparrow}^{NS} + G_{\uparrow\rightarrow\downarrow}^{NS} G_{\uparrow\rightarrow\downarrow}^{NS} \right) \otimes \hat{\sigma}_4 \\ &\quad + 2 \sum_{u,d} \left(G_{\uparrow\rightarrow\uparrow}^{NS} G_{\uparrow\rightarrow\downarrow}^{NS} + G_{\uparrow\rightarrow\downarrow}^{NS} G_{\uparrow\rightarrow\uparrow}^{NS} \right) \otimes (\hat{\sigma}_{NS}^{\Sigma} + \hat{\sigma}_4),\end{aligned}\tag{55}$$

where $\hat{\sigma}_{NS}^{\Sigma}$ is given in (46). Now there is a ‘‘direct’’ contribution to σ_{++}^{NS} coming from $\hat{\sigma}_4$. However, this contribution is small and the primary higher order contribution comes from the $\tilde{\sigma}_1$ correction to $\hat{\sigma}_{NS}^{\Sigma}$ in the ‘‘indirect’’ contribution.

3.3 Spin Asymmetry A_{LL}

The non-singlet spin asymmetry parameter A_{LL}^{NS} is defined by,

$$A_{LL}^{NS} = \frac{\sigma_{++}^{NS} - \sigma_{+-}^{NS}}{\sigma_{++}^{NS} + \sigma_{+-}^{NS}} = \frac{\sigma_{NS}^{LL}}{\sigma_{NS}^{\Sigma}},\tag{56}$$

and from (45) and (47) see that

$$A_{LL}^{NS} = \frac{\sum_{q=u,d} \left(\Delta G_{p\rightarrow q}^{NS} \Delta G_{p\rightarrow q}^{NS} \right) \otimes \hat{\sigma}_{NS}^{LL}}{\sum_{q=u,d} \left(G_{p\rightarrow q}^{NS} G_{p\rightarrow q}^{NS} \right) \otimes \hat{\sigma}_{NS}^{\Sigma}}.\tag{57}$$

Equation (52) implies that to leading order at the parton level,

$$\hat{\sigma}_{NS}^{LL} = -\hat{\sigma}_{NS}^{\Sigma} \quad \text{and} \quad \hat{A}_{LL}^{NS} = -1 \quad (\text{leading order}).\tag{58}$$

We can make a “zero order” estimate of A_{LL}^{NS} by simply ignoring the convolution in (57) and using (58) which results in

$$A_{LL}^{NS}(\text{order } 0) = -\frac{(\frac{4}{9})\Delta G_{p \rightarrow u}^{NS}\Delta G_{p \rightarrow u}^{NS} + (\frac{1}{9})\Delta G_{p \rightarrow d}^{NS}\Delta G_{p \rightarrow d}^{NS}}{(\frac{4}{9})G_{p \rightarrow u}^{NS}G_{p \rightarrow u}^{NS} + (\frac{1}{9})G_{p \rightarrow d}^{NS}G_{p \rightarrow d}^{NS}}. \quad (59)$$

Fig. 12 shows this ratio of parton distributions at $Q = M = 10$ GeV versus x . The result is compared with the complete leading order and beyond leading order predictions for A_{LL}^{NS} from (57), integrated over y at $W = 200$ GeV plotted versus x_T . At $Q = 10$ GeV the leading order and the beyond leading order results are almost identical and both resemble the zero order estimate.

Fig. 13 shows the leading and beyond leading order results for the non-singlet asymmetry parameter A_{LL}^{NS} for proton-proton collisions at $W = 200$ GeV and $Q = M = 2$ GeV. The asymmetry is around 15% between p_T of 2 and 8 GeV and there is very little difference between the leading and beyond leading order. As can be seen in Fig. 6 and Fig. 7, the K-factor for the asymmetry parameter A_{LL}^{NS} is much smaller than the K-factors for unpolarized or polarized cross sections, σ_{Σ}^{LL} and σ_{NS}^{LL} .

4 Summary and Conclusions

From (46) and (48) we see that to order α_s^2 at the parton level,

$$-\hat{\sigma}_{NS}^{LL} = \hat{\sigma}_{NS}^{\Sigma} + 2\hat{\sigma}_4, \quad (60)$$

which means that except small differences due to the term $\hat{\sigma}_4$ and small differences arising from the fact that the polarized parton distributions $\Delta G_{p \rightarrow q}^{NS}$ in (47) differ from the unpolarized one $G_{p \rightarrow q}^{NS}$ in (45), the higher order corrections to polarized cross section, $-\hat{\sigma}_{NS}^{LL}$, and the unpolarized cross section $\hat{\sigma}_{NS}^{\Sigma}$ are identical. In both cases the higher order corrections are large and important. Everything that has previously been said about the higher order corrections to the unpolarized cross section, for example [10], is true for the polarized case as well.

The higher order corrections to the ratio of the polarized to the unpolarized cross section,

$$A_{LL}^{NS} = \sigma_{NS}^{LL}/\sigma_{NS}^{\Sigma}, \quad (61)$$

are small since the big corrections to the numerator are canceled by big corrections to the denominator. As can be seen in Fig. 12 and Fig. 13, A_{LL}^{NS} is very stable against higher order corrections. The asymmetry is around 15% between p_T of 2 and 8 GeV in proton-proton collisions at $W = 200$ GeV and $Q = M = 2$ GeV. The non-singlet asymmetry, A_{LL}^{NS} , is a direct measurement of the non-singlet (*i.e.*, valence) polarized quark distributions within the proton. However, to construct the non-singlet observables in this paper one must subtract pp spin measurements from the corresponding $\bar{p}p$ measurement, and it is unlikely that this will be done in the near

future. On the other hand, if A_{LL} is measured in pp collisions at RHIC, then deviations from our predictions will indicate large contributions from gluons, $\Delta G_{p \rightarrow g}$, and/or from the sea, $\Delta G_{p \rightarrow s}$. This would provide the first hint as to the behavior of the polarized gluon parton distribution, $\Delta G_{p \rightarrow g}$.

Acknowledgements

We warmly thank L. E. Gordon and Cetin Savkli for illuminating discussions.

References

- [1] A. P. Contogouris, B. Kamal, Z. Merebashvili and F. V. Tkachov, Phys. Lett. B304 (1993) 329; Phys. Rev. D48 (1993) 4092, L. E. Gordon and W. Vogelsang, Phys. Rev. D48 (1993) 3136.
- [2] C. Corianò and L. E. Gordon, Nucl. Phys. B469 (1996) 202, Phys. Rev. D54 (1996) 781.
- [3] S. Chang, C. Corianò and L. E. Gordon, hep-ph/9709496.
- [4] J. Ralston and D. Soper, Nucl. Phys. B152 (1979) 109.
- [5] S. Chang, C. Corianò and J. K. Elwood, hep-ph/9709476.
- [6] S. Chang, C. Corianò, R. D. Field, L. E. Gordon, hep-ph/9705249, to appear on Nucl. Phys. B; Phys. Lett. B403 (1997) 344.
- [7] P. Ratcliffe, Nucl. Phys. B223 (1983) 45.
- [8] T. Gehrmann, Nucl. Phys. B498 (1997) 245.
- [9] T. Gehrmann, W. J. Stirling, Phys. Rev. D53 (1996) 6100.
- [10] R. K. Ellis, G. Martinelli and R. Petronzio, Nucl. Phys. B211 (1983) 106.

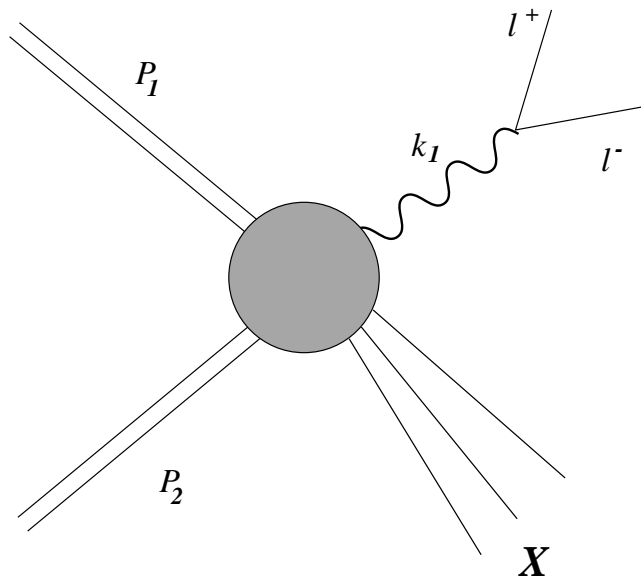


Figure 1: The Drell-Yan Process.

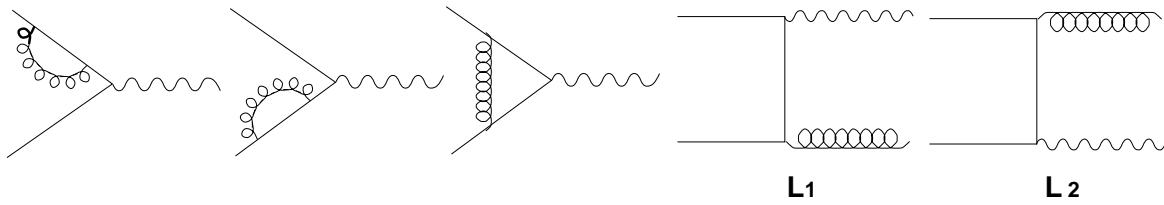


Figure 2: Radiative corrections at $p_T = 0$ and the lowest order contributions at $p_T \neq 0$.

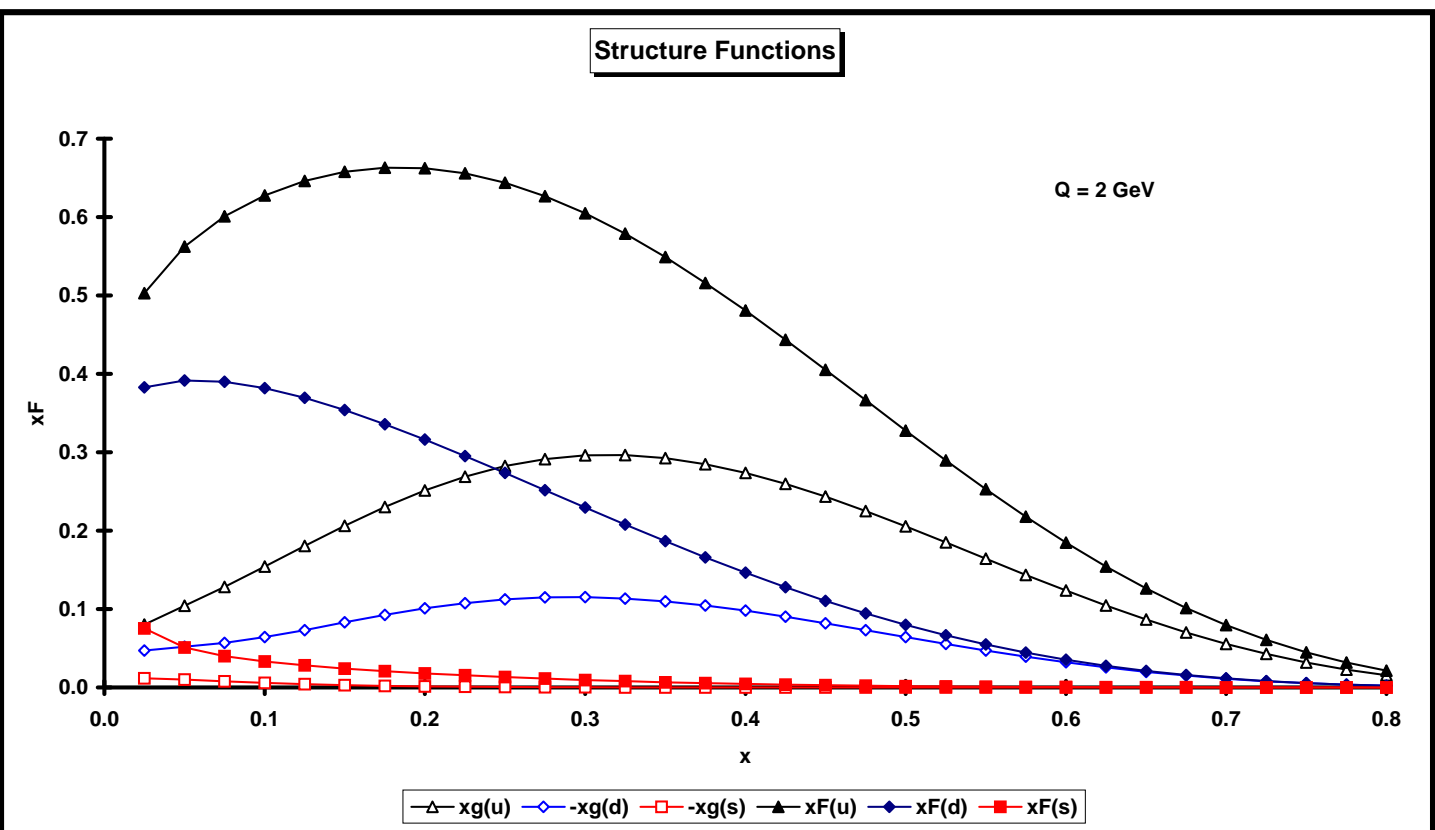


Figure 3: Polarized (xg) and unpolarized (xF) structure functions at $Q = 2$ GeV from Ref.[9] (LO solution A).

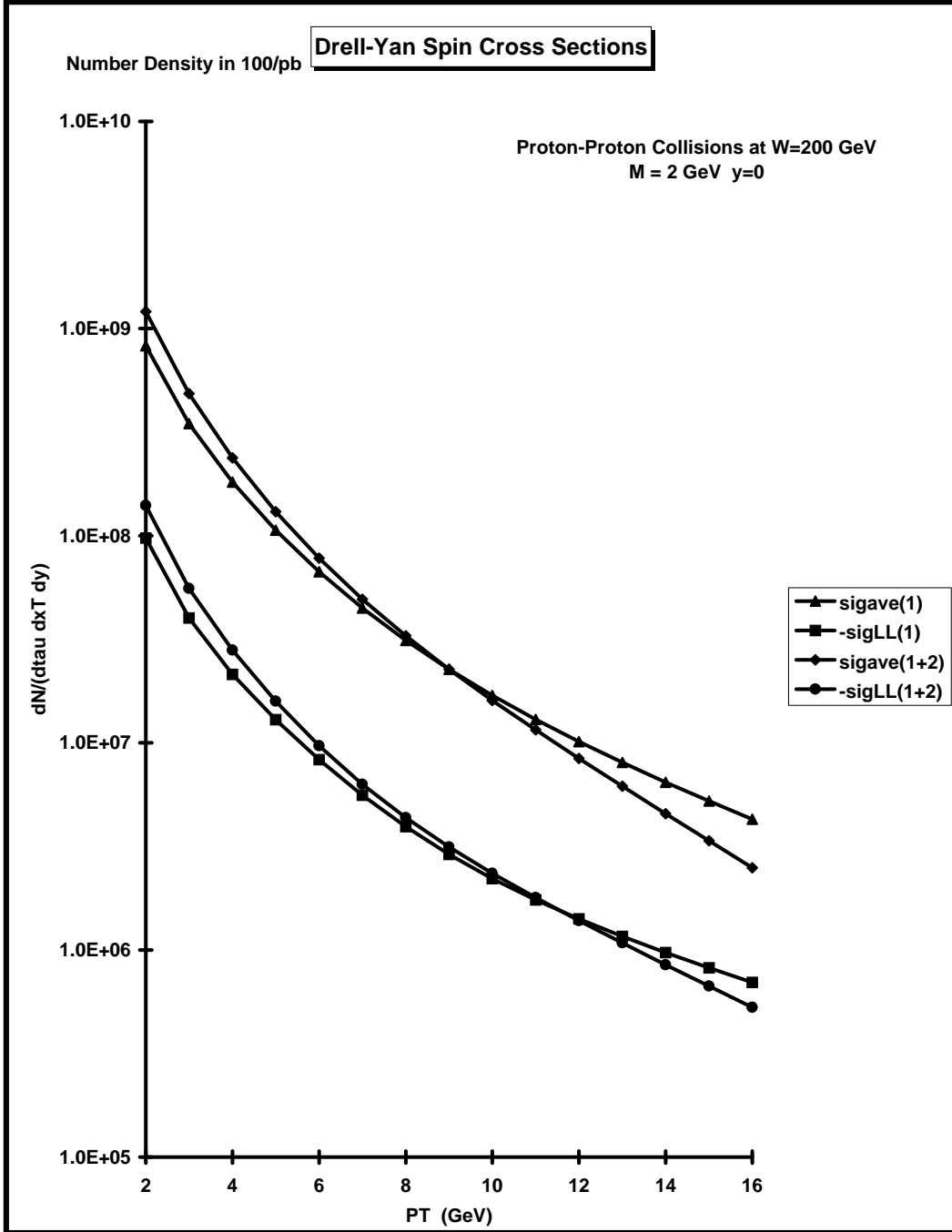


Figure 4: The non-singlet unpolarized spin-averaged (ave) cross section, σ_{NS}^{Σ} , and longitudinally polarized (LL) cross section, σ_{NS}^{LL} , for pp collisions at $W = 200$ GeV, $Q = M = 2$ GeV, and $y = 0$ as a function of p_T . The plot shows the “number density”, $dN/d\tau dx_T dy$, in 100/pb at leading order (1) and at order α_s^2 (1+2).

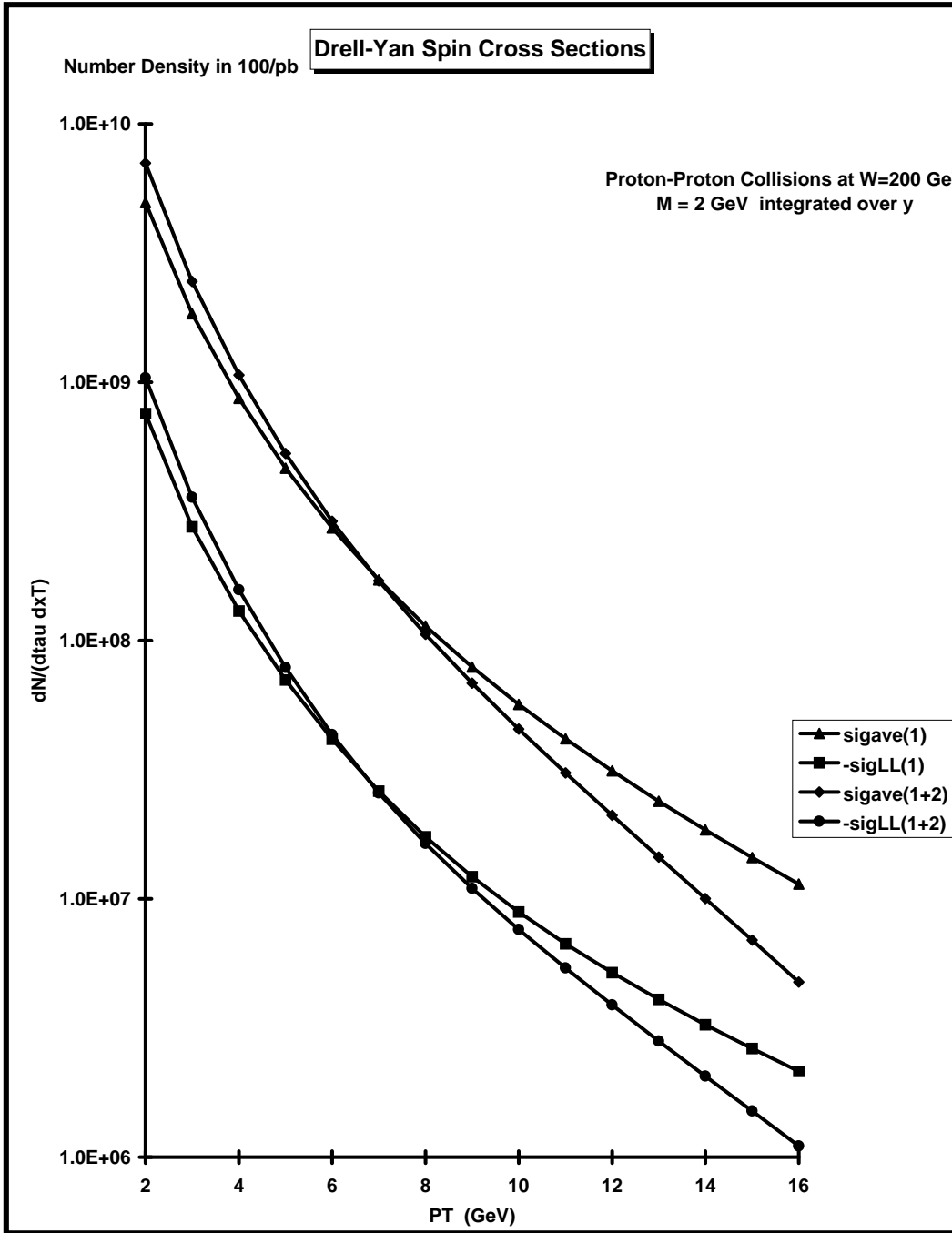


Figure 5: Same as Fig. 4 integrated over rapidity y .

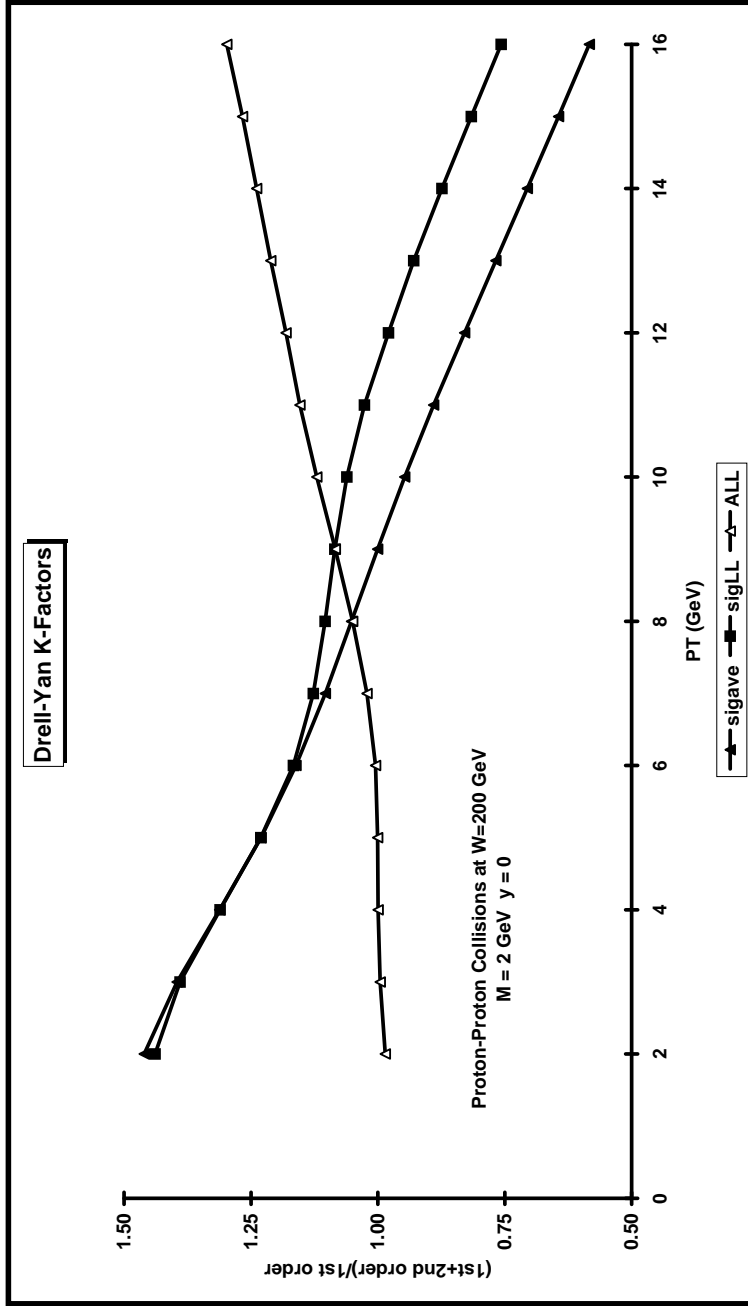


Figure 6: Shows the K -factors for non-singlet unpolarized spin-averaged (ave) and longitudinally polarized (LL) cross sections for pp collisions at $W = 200$ GeV, $Q = M = 2$ GeV, and $y = 0$ as a function of p_T in Fig. 4. The K -factor is the ratio of the full order α_s^2 cross section (1+2) to the leading order Born term (1). Also shown is the K -factor for the non-singlet spin symmetry parameter $A_{LL}^{NS} = \sigma_{NS}^{LL}/\sigma_{NS}^{\Sigma}$.

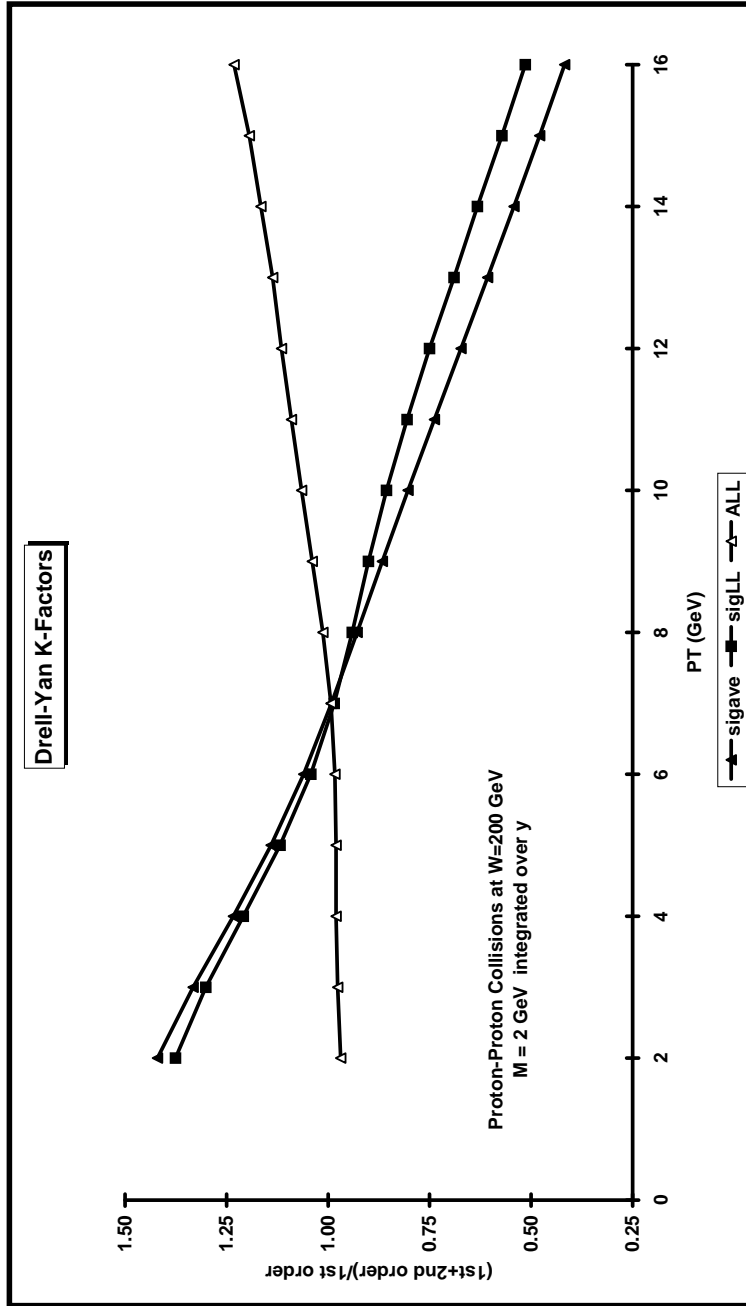


Figure 7: Shows the K -factors for non-singlet unpolarized spin-averaged (ave) and longitudinally polarized (LL) cross sections for pp collisions at $W = 200$ GeV, $Q = M = 2$ GeV, integrated over rapidity y as a function of p_T in Fig. 5. The K -factor is the ratio of the full order α_s^2 cross section (1+2) to the leading order Born term (1). Also shown is the K -factor for the non-singlet spin symmetry parameter $A_{LL}^{NS} = \sigma_{NS}^{LL}/\sigma_{NS}^{\Sigma}$.

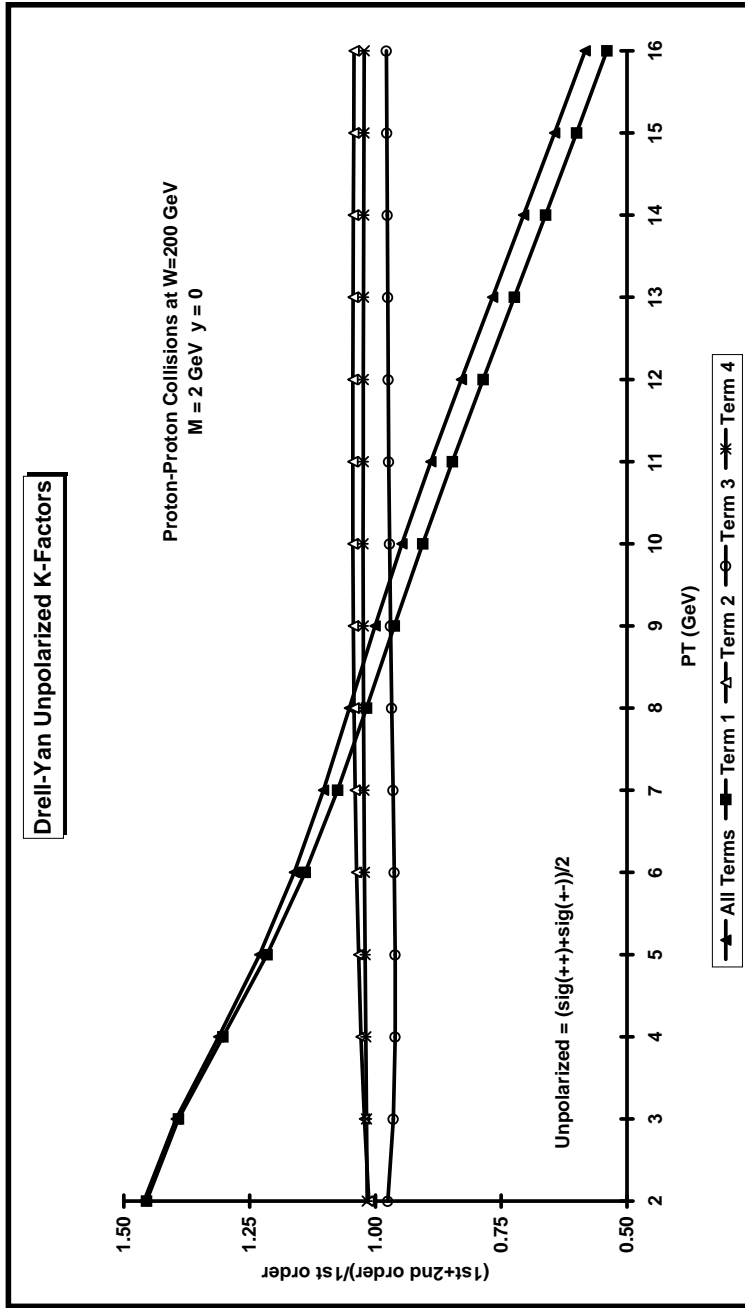


Figure 8: Shows the K -factors arising from each of the four terms in (46) for non-singlet unpolarized spin-averaged cross section, σ_{NS}^{Σ} , for pp collisions at $W = 200$ GeV, $Q = M = 2$ GeV, and $y = 0$ as a function of p_T . The K -factor is the ratio of the order α_s^2 cross section to the leading order Born term.

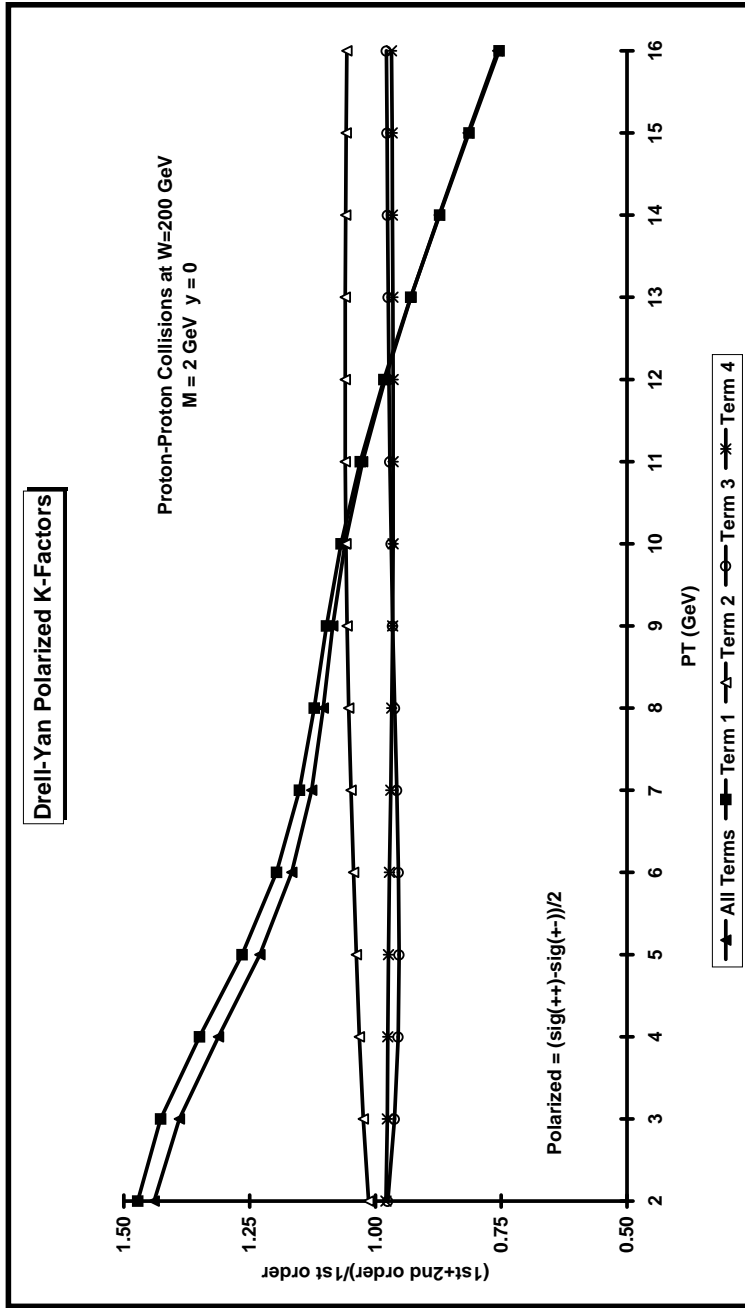


Figure 9: Shows the K -factors arising from each of the four terms in (48) for non-singlet longitudinally polarized (LL) cross section, σ_{NS}^{LL} , for pp collisions at $W = 200$ GeV, $Q = M = 2$ GeV, and $y = 0$ as a function of p_T . The K -factor is the ratio of the order α_s^2 cross section to the leading order Born term.

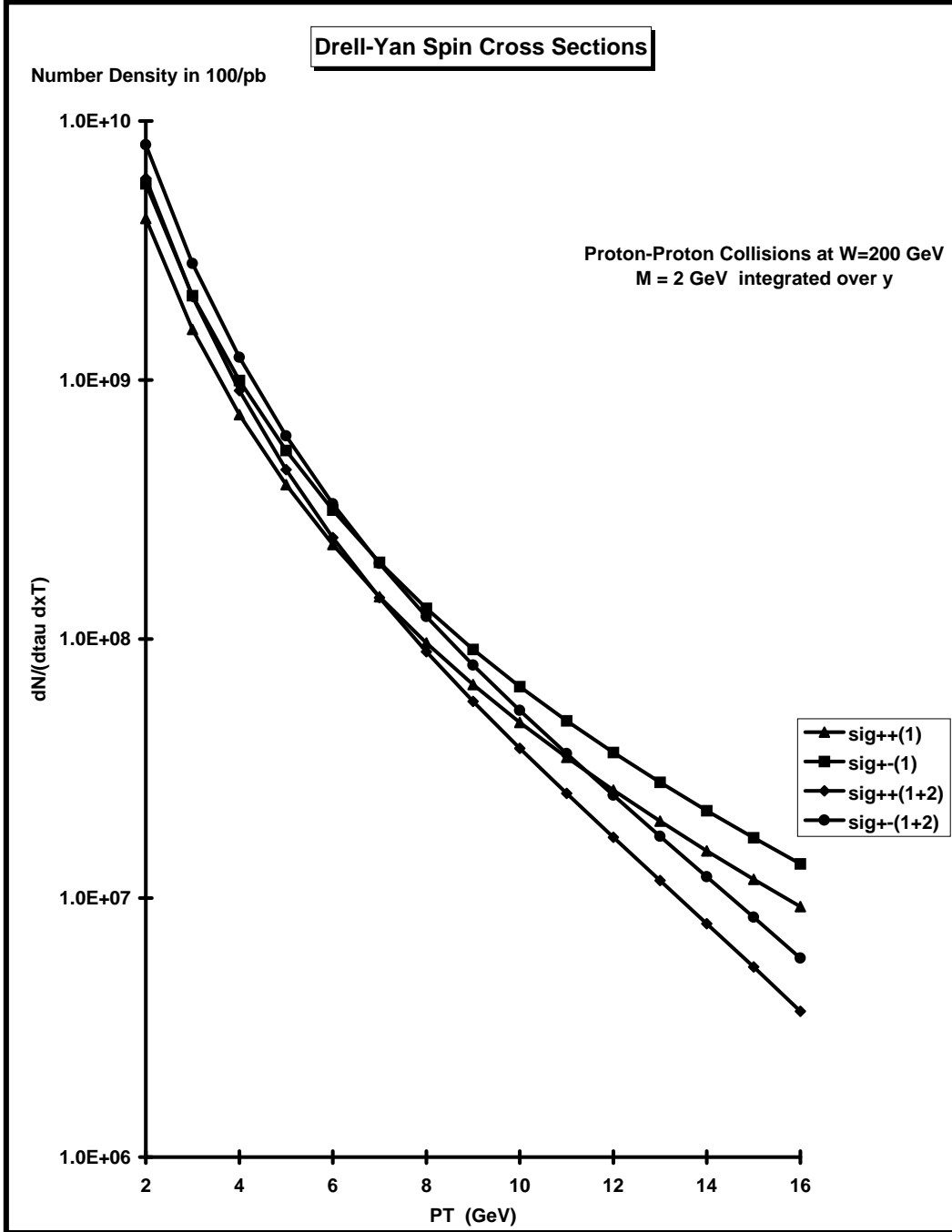


Figure 10: The non-singlet spin cross sections, σ_{++}^{NS} and σ_{+-}^{NS} , for pp collisions at $W = 200$ GeV, $Q = M = 2$ GeV, integrated over y as a function of p_T . The plot shows the “number density”, $dN/d\tau dx_T$, in 100/pb at leading order (1) and at order α_s^2 (1+2).

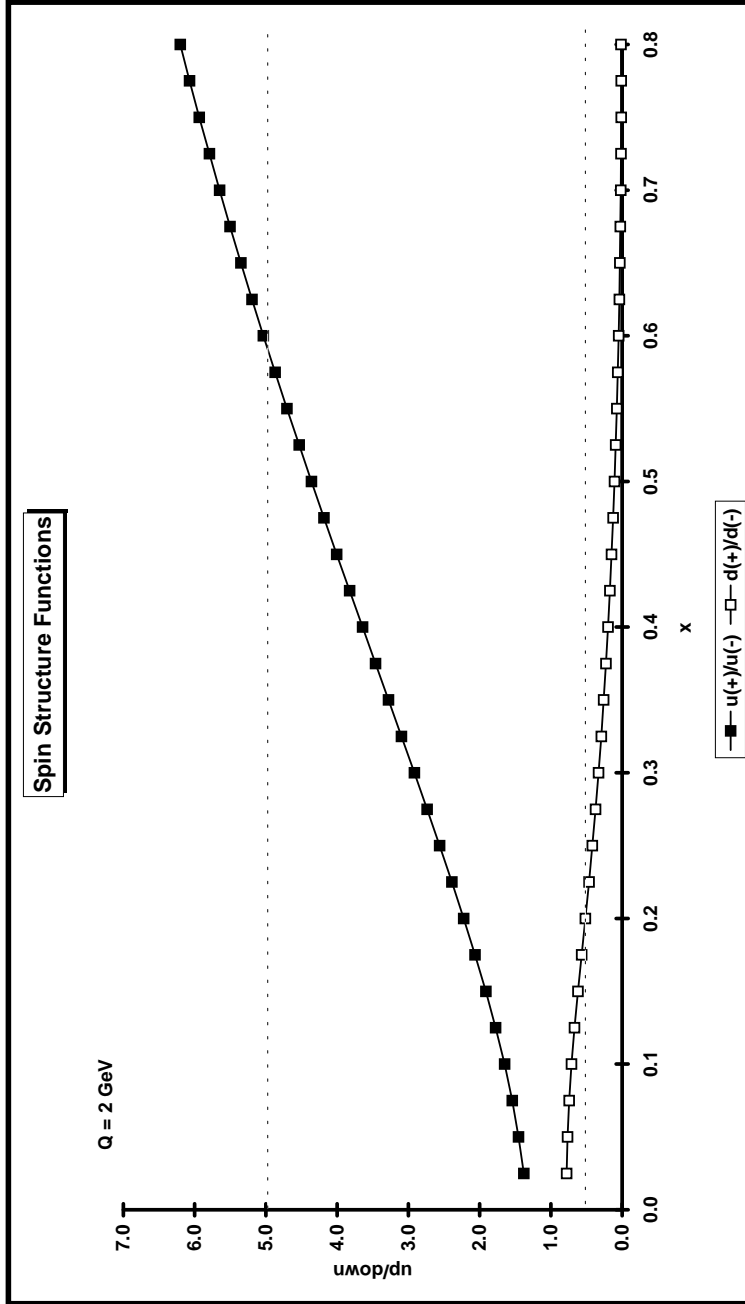


Figure 11: Shows the ratio, $G_{\uparrow\rightarrow\uparrow}/G_{\uparrow\rightarrow\downarrow}$, for u and d quarks at $Q = 2 \text{ GeV}$ versus x resulting from the polarized structure functions in Fig. 3.

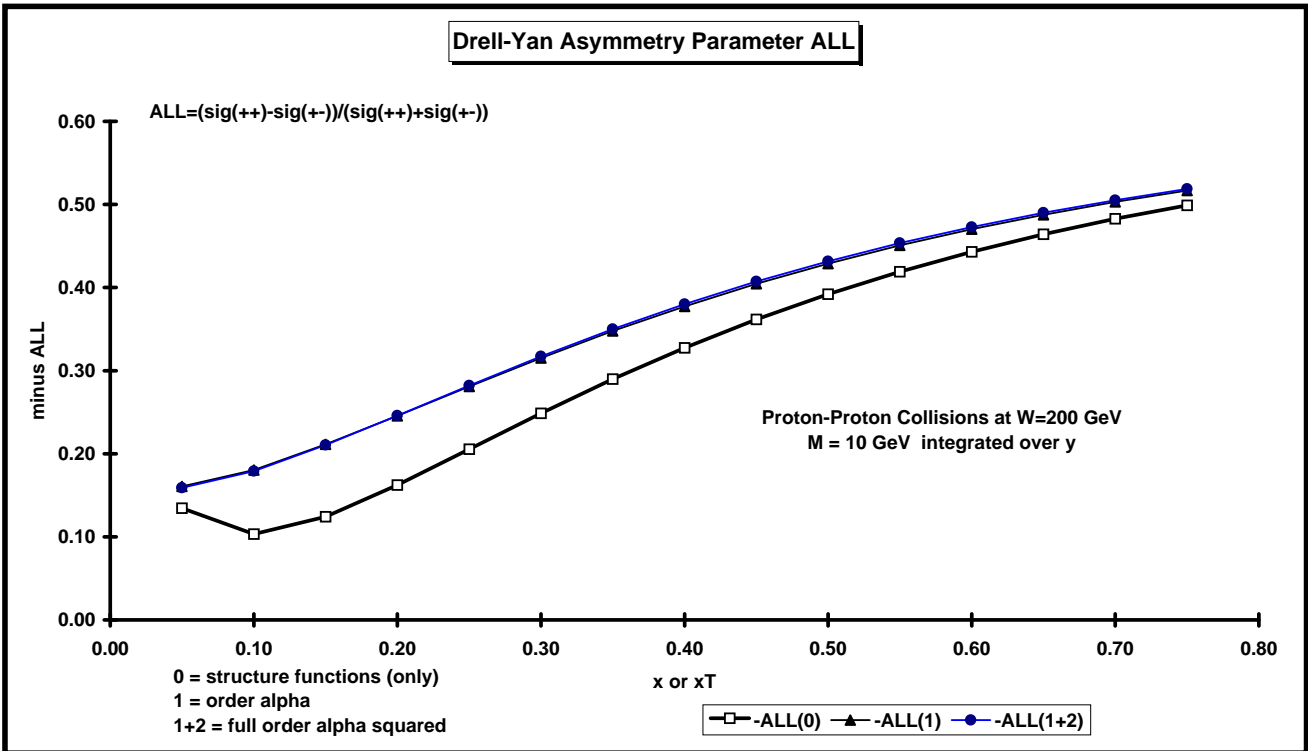


Figure 12: The Drell-Yan non-singlet spin asymmetry parameter $-A_{LL}^{NS} = -\sigma_{NS}^{LL}/\sigma_{NS}^{\Sigma}$ for pp collisions at $W = 200$ GeV, $Q = M = 10$ GeV, integrated over y as a function of x_T at leading order (1) and at order α_s^2 (1+2). Also shown is the “zero order” structure function estimate in (59) plotted versus x (0).

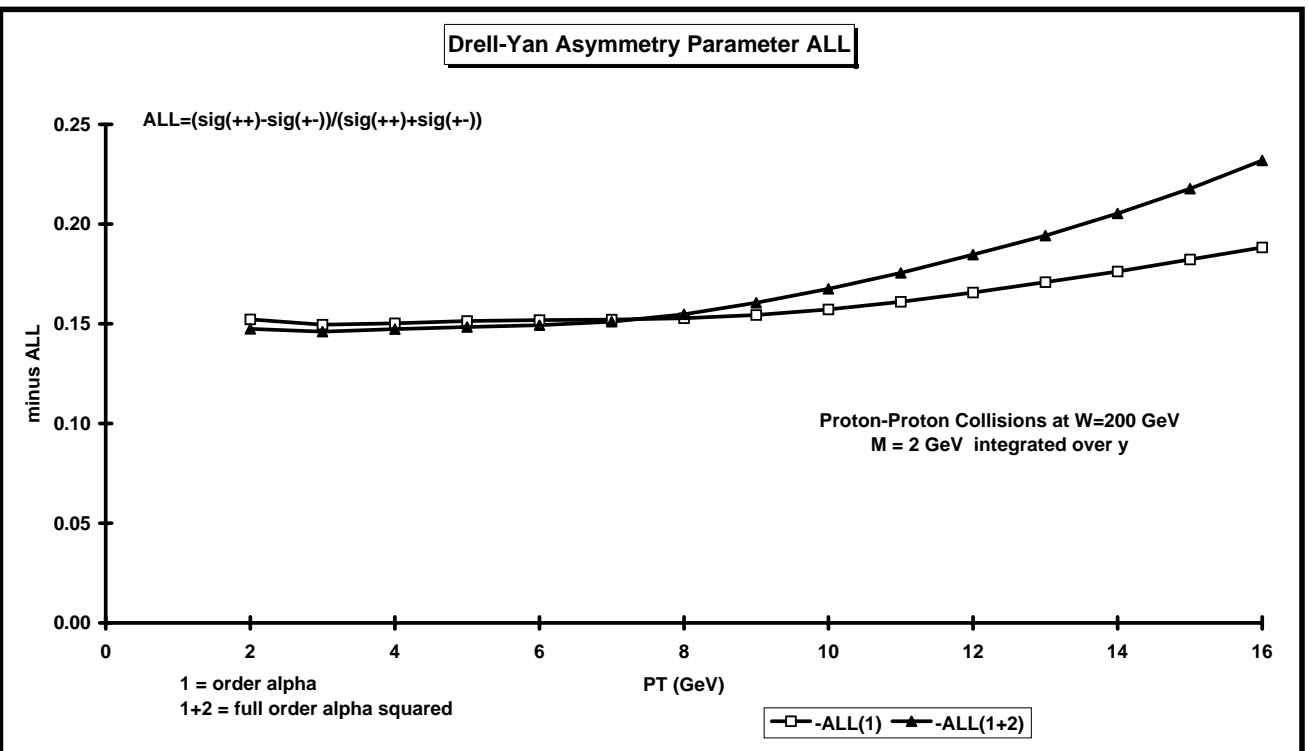


Figure 13: The Drell-Yan non-singlet spin asymmetry parameter $-A_{LL}^{NS}$ = $-\sigma_{NS}^{LL}/\sigma_{NS}^{\Sigma}$ for pp collisions at $W = 200$ GeV, $Q = M = 2$ GeV, integrated over y as a function of p_T at at leading order (1) and at order α_s^2 (1+2).